JOURNAL OF VIROLOGY, Apr. 1999, p. 2803–2813 Vol. 73, No. 4
0022-538X/99/$04.00+0

The Herpes Simplex Virus Type 1 Regulatory Protein ICP27 Is Required for the Prevention of Apoptosis in Infected Human Cells

MARTINE AUBERT AND JOHN A. BLAHO*

Department of Microbiology, Mount Sinai School of Medicine, New York, New York 10029

Received 10 November 1998/Accepted 23 December 1998

The herpes simplex virus type 1 (HSV-1) ICP27 protein is an immediate-early or α protein which is essential for the optimal expression of late genes as well as the synthesis of viral DNA in cultures of Vero cells. Our specific goal was to characterize the replication of a virus incapable of synthesizing ICP27 in cultured human cells. We found that infection with an HSV-1 ICP27 deletion virus of at least three separate strains of human cells did not produce immediate-early or late proteins at the levels observed following wild-type virus infections. Cell morphology, chromatin condensation, and genomic DNA fragmentation measurements demonstrated that the human cells died by apoptosis after infection with the ICP27 deletion virus. These features of the apoptosis were identical to those which occur during wild-type infections of human cells when total protein synthesis has been inhibited. Vero cells infected with the ICP27 deletion virus did not exhibit any of the features of apoptosis. Based on these results, we conclude that while HSV-1 infection likely induced apoptosis in all cells, viral evasion of the response differed among the cells tested in this study.

Herpes simplex virus type 1 (HSV-1) is a neurotropic herpesvirus which causes a variety of infections in humans. It remains latent in the neurons of its host for life and can be reactivated to cause lesions at or near the initial site of infection. Recurrent infections result from the lytic replication of the virus after reactivation from the latent state. During a productive infection in cultured cells, HSV-1 gene expression proceeded in a tightly regulated cascade (15, 16). Changes in the levels of gene expression in HSV-1-infected cells were usually the consequence of transcriptional regulation (36). The first viral genes expressed during infection were transcribed in the absence of de novo viral protein synthesis (4), and they were termed the α, or immediate-early (IE), genes. The α gene products ICP0, -4, -22, and -27 have regulatory functions, and they cooperatively act to regulate the expression of all classes of viral genes (reviewed in reference 36). The β, or early (E), genes were expressed next and encode many of the proteins involved in viral DNA synthesis (15, 16). The last set of genes expressed were the γ, or late (L), genes, and they mainly encode virion components such as VP16 (4).

HSV-1 is a member of a family of cytolytic viruses whose lytic replication cycle ultimately leads to the destruction of cells in culture. The cytopathic effect (CPE) of HSV-1 infection was generally observed as the rounding up of cells almost immediately upon infection, and it tended to become more severe with increasing times of infection (33). Manifestations of HSV-1 infection included (i) the loss of matrix binding proteins on the cell surface, leading to detachment; (ii) modifications of membranes; (iii) cytoskeletal destabilizations; (iv) nucleolar alterations; and (v) chromatin margination and aggregation or damage, as well as (vi) a decrease in cellular macromolecular synthesis (2, 11, 14, 33–35). While it was clear that productive HSV-1 infection caused major biochemical alterations within the infected cells, which had various structural ramifications, the exact method by which the virus actually killed the cells was not well understood.

The observed death of cells following infection with wild-type HSV-1 likely resulted from some form of virus-induced necrosis leading to the classic manifestations of CPE. This cytopathology was a consequence of the virus "taking over the cell" in order to perform its replication cycle, as well as the presence of toxic viral gene products. For example, it was shown that the product of the HSV-1 U_L41 gene, which is packaged in the virion (31), functioned to degrade host mRNA early in infection (9). This feature of HSV-1, that it encodes gene products which might directly injure host cells, has limited the development of the virus as a gene transfer vehicle. Accordingly, most current research efforts in this area have focused on limiting the synthesis of viral proteins in an attempt to reduce cell toxicity (17, 18, 38, 39, 46).

It was also shown that HSV-1 infection could induce programmed cell death through at least two separate pathways which were distinct from the necrotic route described above. Initially, cell death caused by the complete blockage of protein synthesis induced during infection was shown to be inhibited by the product of the $\gamma_1$34.5 gene (7), which functions to block the phosphorylation of the eIF-2α translation factor (8, 13). Recently, Koyama and Adachi (20) showed that wild-type HSV-1 infection could also induce apoptosis under conditions in which de novo viral protein synthesis was inhibited, suggesting that (i) induction was likely an early event and (ii) HSV-1 produced polypeptides which specifically blocked apoptosis. In addition, HSV-1 also blocked apoptosis which was induced by sorbitol-mediated osmotic shock (21), hypothermia and thermal shock (22), or exposure to ceramide, tumor necrosis factor, and anti-FAS antibody (10). While these studies, when taken together, suggested that HSV-1 induction of apoptosis occurred almost immediately upon infection, it was reported that the early viral protein kinase U_S3 was one of the gene products required for blocking this effect (23).

As the genome of HSV-1 encodes over 80 unique gene

* Corresponding author. Mailing address: Department of Microbiology, Mount Sinai School of Medicine, One Gustave L. Levy Pl., New York, NY 10029. Phone: (212) 241-7318. Fax: (212) 534-1684. E-mail: blaho@msvax.mssm.edu.

products, the generation of recombinant viruses containing specific deletions (29) of individual HSV-1 genes has been an enormously useful technique for the elucidation of the function of viral proteins in HSV-1 replication. Our study focused on the α regulatory protein ICP27. Previous experiments with mutant recombinant viruses unable to produce functional ICP27 (ICP27 null) showed that ICP27 was essential for the optimal expression of L genes, as well as the synthesis of viral DNA (25, 32, 37, 43–45). These studies were performed in cultures of Vero cells, which are of African green monkey origin. Thus, our specific goal was to use one of these ICP27-null viruses (44) to determine the role which ICP27 plays in the replication of HSV-1 in cultured human cells.

In this study, we report that for at least three separate strains of human cells (HEp-2, HeLa, and 143tk$^-$), infection with an HSV-1 ICP27-null virus did not produce IE or L proteins at the levels observed following wild-type virus infections of these cells. Measurements of cell morphology, chromatin condensation, and genomic DNA fragmentation demonstrated that the human cells died by apoptosis after infection with the ICP27-null virus. The features of the apoptosis in these human cells were identical to those which occur during wild-type infections in human cells when total protein synthesis has been inhibited. Infections of Vero or Vero 2.2 cells with the ICP27 deletion virus did not exhibit any of the features of apoptosis. Based on these results, we conclude that while HSV-1 infection likely induced apoptosis in all cells, viral evasion of the response differed among the cells tested in this study.

MATERIALS AND METHODS

Cells and viruses. All cells were maintained in Dulbecco's modified Eagle's medium (DMEM) containing 5% fetal bovine serum. Human HEp-2, 143tk$^-$, and HeLa cells and nonhuman Vero cells were obtained from the American Type Culture Collection (Rockville, Md.). Vero 2.2 cells and the KOS1.1, vBSΔ27, and vBSΔ27R viruses were generously provided by Saul Silverstein (Columbia University). Vero 2.2 is a derivative Vero cell line expressing ICP27 under its own promoter (43). KOS1.1 was the strain of wild-type HSV-1 used in this study. vBSΔ27 was the ICP27-null mutant virus used in this analysis; it contains a replacement of the α27 gene with the *Escherichia coli lacZ* gene and therefore must be propagated on an ICP27-complementing cell line, such as Vero 2.2 (43). In addition, no extraneous mutations outside the α27 allele were introduced during the generation of the virus (44). vBSΔ27R was derived from vBSΔ27 after repairing the α27 deletion (44), and therefore, it was also used as a control wild-type virus. In all cases, the cell monolayers were infected at a multiplicity of infection of 10, and the infections proceeded at 37°C in DMEM containing 5% newborn calf serum for the times indicated in the text.

Extraction of infected cells and immunoblotting analyses. Whole extracts of infected cells were obtained as follows. Cells were scraped into the medium and collected following low-speed centrifugation. After being washed with phosphate-buffered saline containing protease inhibitors [0.1 mM phenylmethylsulfonyl fluoride, 0.1 mM L-1-chlor-3-(4-tosylamido)-4-phenyl-2-butanone (TPCK), 0.01 mM L-1-chlor-3-(4-tosylamido)-7-amino-2-heptanon-hydrochloride (TLCK)], the infected cells were lysed in a solution containing 50 mM Tris-HCl, pH 7.5, 150 mM NaCl, 5 mM EDTA, 0.4% Triton X-100, 0.1 mM phenylmethylsulfonyl fluoride, 0.1 mM TPCK, 0.01 mM TLCK (buffer A) and sonicated with a Branson sonifier. The protein concentrations of all cell extracts were determined by a modified Bradford protein assay (Bio-Rad Laboratories). Equal amounts of infected cell proteins (50 μg) were separated in denaturing 12% *N,N′*-diallyltartardiamide-acrylamide gels and electrically transferred to nitrocellulose membranes in a tank apparatus (Bio-Rad) prior to immunoblotting. The following antibodies were used for the immunoblotting experiments: (i) RGST22, rabbit polyclonal antibody specific for full-length ICP22 (6); (ii) 1113, mouse anti-ICP27 monoclonal antibody (Goodwin Institute for Cancer Research, Plantation, Fla.); (iii) 1114, mouse anti-ICP4 monoclonal antibody (Goodwin); (iv) 1112, mouse anti-ICP0 monoclonal antibody (Goodwin); and (v) VP16 (1-21), mouse anti-VP16 monoclonal antibody (Santa Cruz Biotechnology, Inc.). Secondary (goat) anti-rabbit or anti-mouse antibody conjugated with the alkaline phosphatase was purchased from Southern Biotech (Birmingham, Ala.).

Inhibition of protein synthesis and low-molecular-weight DNA laddering analyses. To inhibit protein synthesis in infected cells, cycloheximide (CHX) (Sigma) was added to the medium of monolayer cultures of Vero and HEp-2 cells at final concentrations of 100 μg/ml and 10 μg/ml, respectively. The cells were pretreated with CHX for 1 h prior to infection. To analyze DNA fragmentation in cells infected in the absence or presence of CHX, low-molecular-weight DNA molecules were isolated from the cells after 6, 9, 12, 15, and 24 h postinfection (p.i.), as described by Koyama and Miwa (21). The DNA samples were subjected to electrophoresis in a horizontal 1.5% agarose gel, stained with ethidium bromide (10 μg/ml), visualized by UV light transillumination, and photographed with Polaroid 667 film.

Microscopy analysis and computer graphics. The phenotypes of the infected cells were documented by phase-contrast light microscopy with an Olympus CK2/PM-10AK3 system with an attached 35-mm camera. For analyses of chromatin condensation, cells were grown and infected (as described above) in a 35-mm-diameter plate (six-well dish) containing a glass coverslip. At 10 and 24 h p.i. the cells were fixed with 2% formaldehyde in PBS for 20 min, permeabilized with 100% acetone at −20°C for 4 min, and incubated with the DNA dye Hoechst 33258 (Sigma) at a final concentration of 0.05 μg/ml in phosphate-buffered saline for 10 min. Photographic images of mounted cells were obtained with a Leica fluorescent microscope. Immunoblots, autoradiograms, photographs, and 35-mm slides were digitized at 600- to 1,200-dot per inch resolution with an AGFA Arcus II scanner linked to a Macintosh G3 PowerPC workstation. Raw digital images, saved as tagged image files with Adobe Photoshop version 5.0, were organized into figures with Adobe Illustrator version 7.1. Grey-scale or color prints of figures were obtained with a Codonics dye sublimation printer.

RESULTS

Differing morphologies of vBSΔ27-infected cell monolayers. The goal of this study was to analyze the replication of an ICP27-null (44) recombinant HSV-1 strain (vBSΔ27) in cultured human cells. Initially, we were interested in directly comparing the cytopathic effects of the ICP27-null virus replication in human cells with that in Vero cells, since some mutant viruses, especially those carrying mutations in genes encoding IE proteins (3, 42, 47), were shown to have phenotypes which varied with the type of cell line or tissue used for the infections. Monolayer cultures of either Vero and Vero 2.2 (nonhuman) or 143tk$^-$, HEp-2, and HeLa (human) cells were mock infected or infected with vBSΔ27, KOS1.1, or vBSΔ27R as described in Materials and Methods. Since vBSΔ27R is a direct repair of vBSΔ27 (44), it was considered a wild-type virus throughout these studies. Vero 2.2 cells are ICP27-expressing Vero cells (43). At 24 h p.i., the effect of the virus on the morphology of each cell type was observed by phase-contrast microscopy (Fig. 1).

The cell morphologies observed after infection of the ICP27-expressing Vero 2.2 cells with either vBSΔ27, KOS1.1, or vBSΔ27R were identical (Fig. 1A, C, and E). The cells appeared to be smooth and rounded, and they tended to lose obvious cell-cell contacts. This general phenotype is defined as the CPE due to viral replication. At 24 h p.i., the corresponding mock-infected Vero 2.2 cells were observed to be a confluent cell monolayer (Fig. 1G), and they presented no sign of CPE. When the infections were performed in Vero cells, cell morphologies the same as those described for the infected Vero 2.2 cells were observed when the KOS1.1 or vBSΔ27R viruses were used (compare Fig. 1D and F with Fig. 1C and E) but not following vBSΔ27 infection (Fig. 1B). The vBSΔ27-infected Vero cells showed a morphology very similar to that of the confluent monolayer of flat cells observed in the mock-infected Vero cells (compare Fig. 1B with Fig. 1H). These results are consistent with the data described by Soliman et al. (44), who showed that vBSΔ27 did not grow and replicate its DNA in Vero cells while it produced the same yield of virus as the wild-type KOS1.1 in Vero 2.2 cells. Thus, the CPE which was observed in infected Vero 2.2 cells and vBSΔ27R- or KOS1.1-infected Vero cells was likely the result of virus replication which did not occur in vBSΔ27-infected Vero cells because of the inability of the mutant virus to replicate in these cells.

For each human cell type (Fig. 1I to T), the morphologies of KOS1.1- and vBSΔ27R-infected monolayers were similar (compare Fig. 1L to N with Fig. 1O to Q) and they corresponded to smooth, rounded cells with reduced cell-cell con-

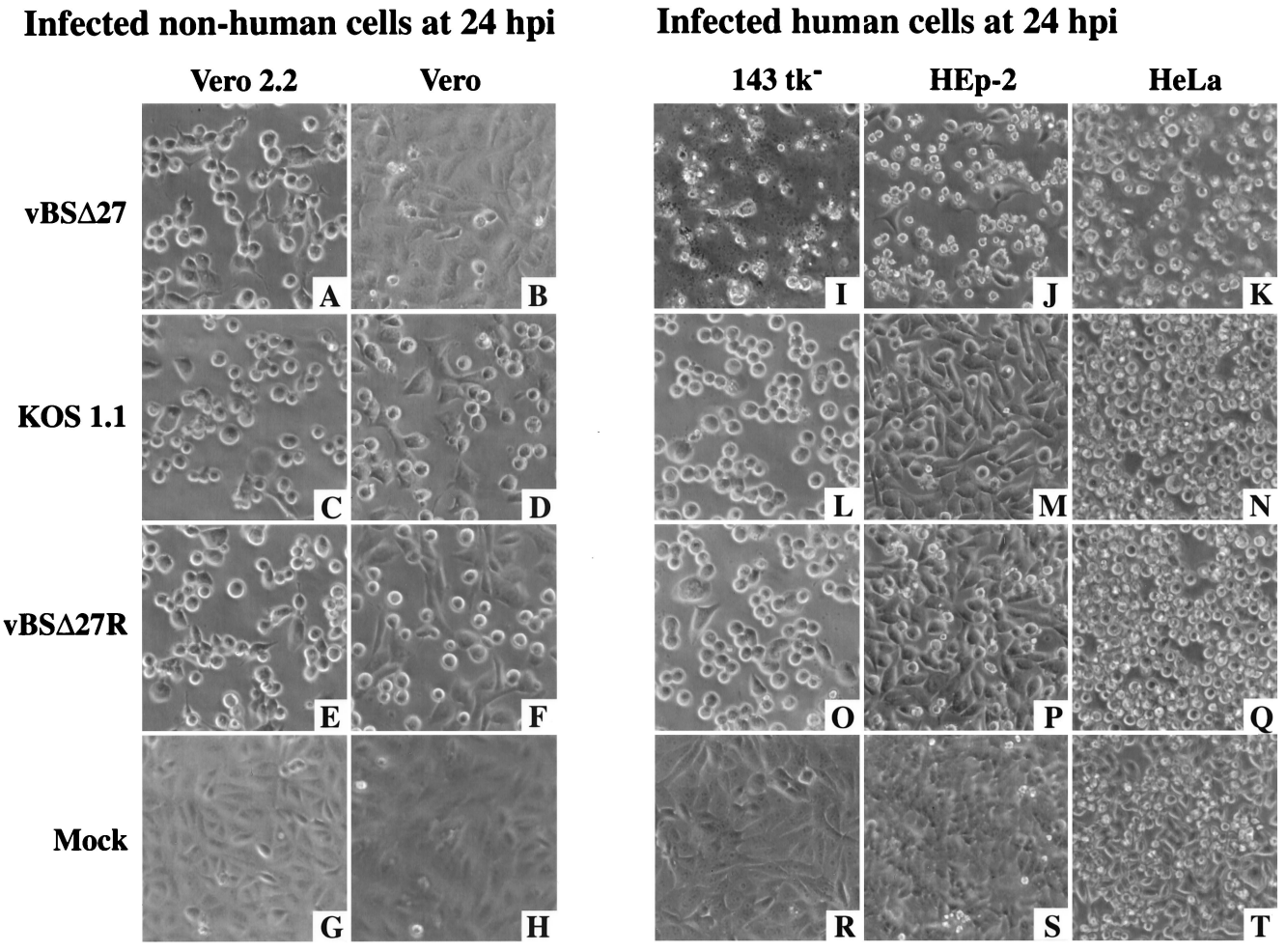

FIG. 1. Morphologies of infected nonhuman (A to H) Vero 2.2 and Vero cells and human (I to T) 143tk$^-$, HEp-2, and HeLa cell lines. Cells infected with vBSΔ27 (A, B, and I to K), KOS1.1 (C, D, and L to N), or vBSΔ27R (E, F, and O to Q) and mock-infected cells (G, H, and R to T) were observed at 24 h p.i. by phase-contrast light microscopy (magnification, ×20) as described in Materials and Methods.

tacts, as observed with Vero and Vero 2.2 cells (Fig. 1C to F). However, infections of the same human cells with vBSΔ27 led to phenotypes (Fig. 1I to K) which were dramatically different from the corresponding KOS1.1- or vBSΔ27R-infected-cell phenotypes (Fig. 1L to Q), as well as the corresponding mock-infected-cell phenotypes (Fig. 1R to T). Each human vBSΔ27-infected cell appeared as novel, irregular shaped, and smaller compared to the cells infected with wild-type viruses. Moreover, most of these vBSΔ27-infected human cells were floating in the medium at 24 h p.i. (data not shown) while those infected with either vBSΔ27R or KOS1.1 remained attached to the flask. These observations suggest that while the human cells were dying after infection with vBSΔ27, their death seemed to proceed through a different route than the one which led to the classical CPE observed with cells infected with wild-type virus.

Reduced accumulations of IE protein ICP22 and L protein VP16 in vBSΔ27-infected human cells at 24 h p.i. The cell morphologies documented in Fig. 1 suggested that the process of human cell death following vBSΔ27 infection differed from that of both wild-type virus infection of human cells and vBSΔ27 infection of Vero cells. One possible explanation for this effect is that the vBSΔ27 virus was able to produce or induce polypeptides which are toxic to the cells (17, 18, 38, 39, 46). To address this possibility, whole extracts were prepared from each infected cell culture shown in Fig. 1, polypeptides were separated in denaturing gels, and the accumulation of the IE protein ICP22 as well as the L protein VP16 at 24 h p.i. was analyzed by immunoblotting as described in Materials and Methods. Due to the observation (Fig. 1) that a large number of vBSΔ27-infected human cells detached from the dishes, exactly equal amounts of infected cell polypeptides were loaded in each lane of the denaturing gel.

The results of this analysis (Fig. 2) showed that in vBSΔ27-infected Vero 2.2 cells, the accumulation of ICP22 or VP16 was similar to that observed with the wild-type viruses vBSΔ27R or KOS1.1 (Fig. 2A, compare lanes 2 through 4). Moreover, ICP22 migrated as a highly posttranslationally modified protein which possessed multiple electrophoretic forms in extracts of Vero 2.2 cell infected with wild-type virus or vBSΔ27. Minor irrelevant contaminating species whose origins are unknown were also observed in some mock-infected cells (Fig. 2A, lane 1). When the infections were performed in Vero cells, almost-equal amounts of VP16 were detected for all viruses and an accumulation of the different electrophoretic forms of ICP22 was also observed (Fig. 2B, lanes 2 to 4). However, the vBSΔ27 infections led to a much higher level of ICP22 accumulation than did infections with the wild-type viruses (Fig. 2B, compare

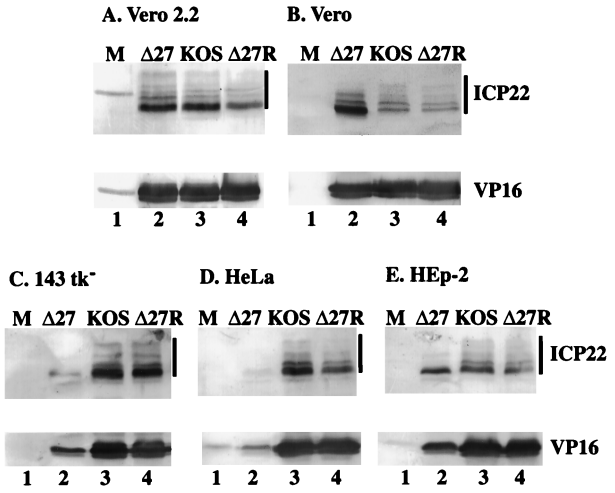

FIG. 2. Accumulation of an IE protein (ICP22) and an L protein (VP16) in infected nonhuman (A and B) and human (C to E) cell lines. Total cell extracts (50 μg) prepared at 24 h p.i. from mock- (M), vBSΔ27 (Δ27)-, vBSΔ27R (Δ27R)-, and KOS1.1-infected nonhuman Vero, Vero 2.2, and human 143tk$^-$, HEp-2, and HeLa cells were used for immunoblot analyses with the polyclonal anti-ICP22 antibody RGST22 and the monoclonal anti-VP16 antibody as described in Materials and Methods. The bars indicate the multiple electrophoretic forms of ICP22.

lane 2 with lanes 3 and 4). Again, this increased accumulation of an IE protein in vBSΔ27-infected Vero cells was consistent with previous studies (44).

When the immunoblot analyses were performed with protein extracts obtained from infected human cells (Fig. 2C to E), lower levels of ICP22 and VP16 were detected for vBSΔ27-infected cells (Fig. 2C to E, lanes 2). We also observed in each of these cells a similar reduction in the levels of synthesis of gD, another viral L (γ_1) protein, following vBSΔ27 infection (data not shown). Meanwhile, KOS1.1 and vBSΔ27R infections (Fig. 2C to E, lanes 3 and 4) led to a level of accumulation of the two proteins similar to that observed with Vero 2.2 and Vero cells (Fig. 2A and B). In addition, while the ICP22 proteins produced by the wild-type viruses migrated as multiple forms, these forms of ICP22 were not observed following vBSΔ27 infection of each type of human cell. Although the levels of ICP22 and VP16 were lower in all of the vBSΔ27-infected human cells, the extent of the reductions varied slightly (HeLa > 143tk$^-$ > HEp-2). This might indicate that among several strains of human cells, the ability to resist the effect caused by vBSΔ27 differs. These results raise the possibility that even cell types of similar origin may exhibit a range of response upon infection.

Our results indicate that at 24 h p.i., while ICP22 accumulated to higher levels in vBSΔ27-infected Vero cells than in cells infected with wild-type viruses, smaller amounts of both ICP22 and VP16 were produced during vBSΔ27 infection of human cells. Since care was taken to insure that equal amounts of infected-cell proteins were loaded in each lane, we conclude that the replication cycle of the vBSΔ27 virus in the human cells was severely compromised at 24 h p.i. Taken together with the cell morphological data shown in Fig. 1, these results suggest that the majority of vBSΔ27-infected human cells were dead at 24 h p.i. We conclude that the mutant virus, but not specific viral protein per se, was toxic to the human cell cultures.

Decreased accumulations of IE and L proteins during the course of vBSΔ27 infections. In the previously described experiments (Fig. 1 and 2), vBSΔ27 infection was studied in several human cells at a single time of infection (24 h). To further characterize the synthesis of viral polypeptides during vBSΔ27 replication, we focused on HEp-2 cells as our prototype human strain. Cell monolayers of the HEp-2 and control Vero cells were infected with vBSΔ27 and KOS1.1, protein extracts were made at different times during the infection, and immunoblotting was performed to follow the postinfection accumulation of four IE proteins (ICP0, -4, -22, and -27) and the L protein VP16 as described in Materials and Methods.

The results (Fig. 3) showed that in HEp-2 cells, the accumulation of ICP0, -4, or -22 or VP16 was detected for both vBSΔ27 and KOS1.1 at 6 h p.i. (Fig. 3A, compare lanes 1 and 5). As expected, ICP27 protein was only observed following KOS1.1 infection. However, at later times p.i. up to 24 h, the amounts of these proteins increased with KOS1.1 (Fig. 3A, lanes 5 to 8) whereas no higher levels of accumulation were

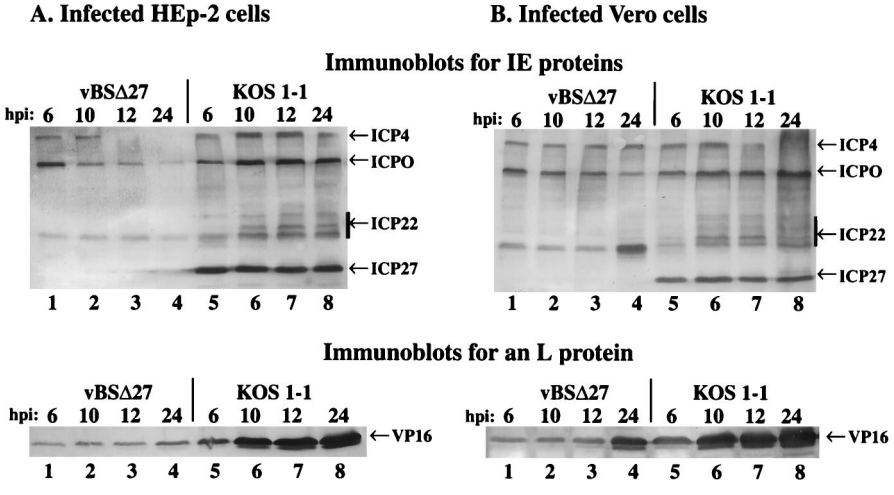

FIG. 3. Accumulation of IE and L proteins in infected cells at various infection times. Total cell extracts (50 μg) prepared at 6, 10, 12, and 24 h p.i. from vBSΔ27- and KOS1.1-infected HEp-2 (A) and Vero (B) cells were used for immunoblot analyses with the polyclonal anti-ICP22 antibody (RGST22), monoclonal anti-ICP4 (1114), anti-ICP27 (1113), anti-ICP0 (1112) antibodies (IE proteins), and the monoclonal anti-VP16 antibody (L protein). IE and L protein locations are shown in the right margins (arrows), and the bars indicate the multiple electrophoretic forms of ICP22.

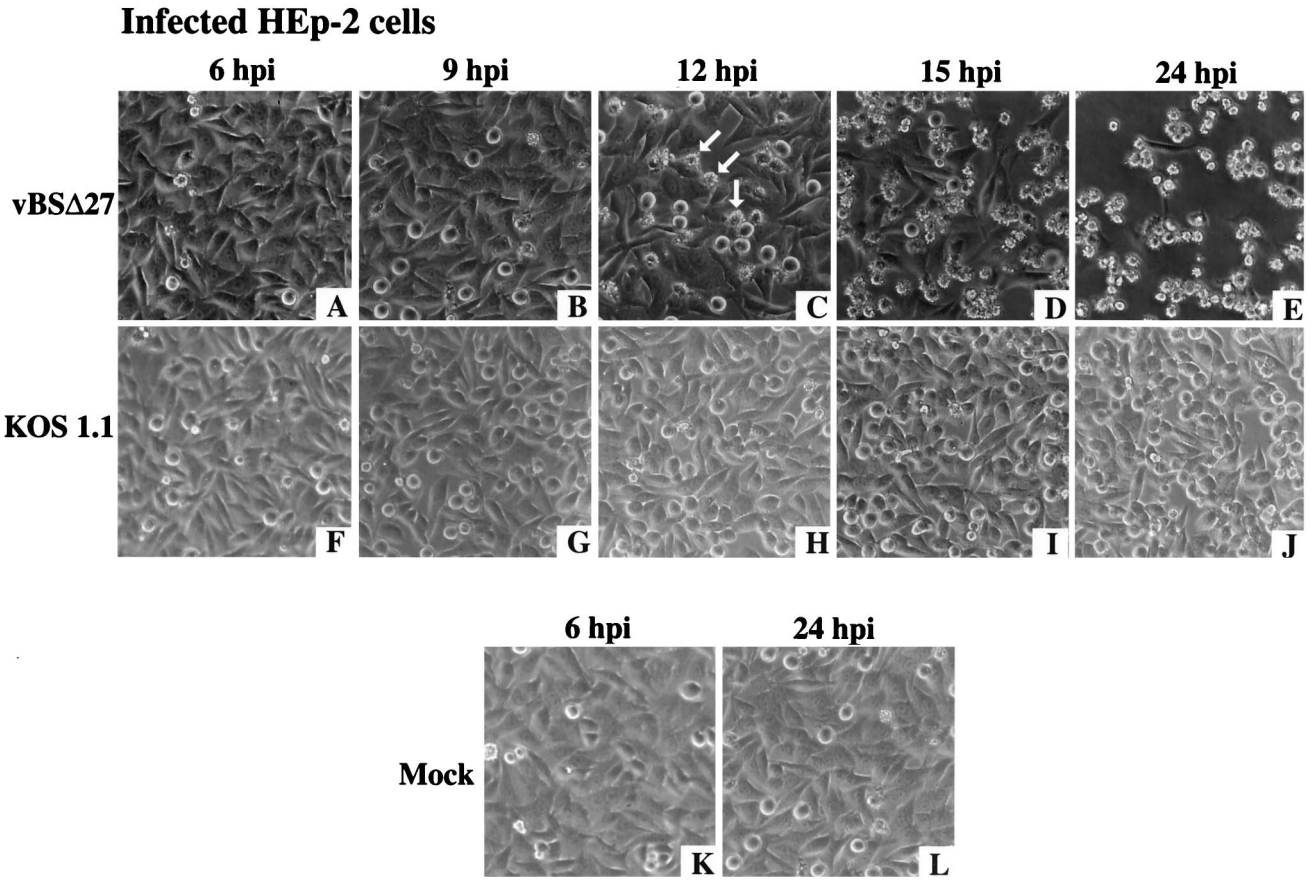

FIG. 4. Morphologic changes during the course of infection in HEp-2 cells. Phase-contrast images of HEp-2 cells infected with vBSΔ27 (A to E) and KOS1.1 (F to J) at 6, 9, 12, 15, and 24 h p.i. were shown. Images of mock-infected cells (K and L) are shown at 6 and 24 h p.i. only. The arrows mark cells possessing the small, irregular phenotypes described in the text. Magnification, ×19.4.

detected with vBSΔ27 (Fig. 3A, lanes 1 to 4). Indeed, in the vBSΔ27-infected HEp-2 cells, the level of VP16 remained at a constant low level while some (ICP4 and ICP0) of the IE protein levels even decreased.

In vBSΔ27-infected Vero cells (Fig. 3B, lanes 1 to 4), accumulations of IE proteins and VP16 (L protein) remained at the same levels from 6 to 12 h p.i. By 24 h p.i., a greater accumulation of both ICP22 and VP16 was detected (Fig. 3B, lane 4). However, the levels of accumulation of VP16 in vBSΔ27-infected Vero cells were not as significant as that observed for the wild-type virus (Fig. 3B, compare lanes 1 to 4 with lanes 5 to 8). Rather, the amount observed at 24 h p.i. was more similar to the amount of VP16 produced by KOS1.1 at 6 h p.i. The levels of ICP4 and ICP0 were either constant or slightly reduced during the vBSΔ27 infection. These results are consistent with those described previously (25, 32, 37, 43, 45), in which mutant viruses defective for ICP27 showed, among their variety of phenotypes, an overabundance of some IE and E proteins combined with reduced levels of L (γ_1) gene products in Vero cells. In addition, multiple electrophoretic forms of ICP22 were observed throughout KOS1.1 infection in Vero cells while only the fastest-migrating form was present at all times of vBSΔ27 infection.

These results showed that the accumulations of the IE and L proteins were basically the same at 6 h p.i. in both vBSΔ27-infected HEp-2 and Vero cells. However, by 10 h p.i., lower levels of IE proteins in the vBSΔ27-infected HEp-2 cells were beginning to be observed, and dramatic differences were seen by 24 h p.i. These events were therefore taking place within a single step of viral replication, suggesting that accumulations of toxic viral components after excessive infection periods (17, 18, 38, 39, 46) were not involved in the process. Thus, we conclude that the consequences of vBSΔ27 infection in human cells occur early in infection and they likely involve a dramatic global change in cell metabolism rather than a specific or targeted effect.

Morphological changes of HEp-2 cells occurring during infection with vBSΔ27 were observed by 12 h p.i. To determine whether the reduction in accumulation of IE and L proteins (Fig. 2 and 3) in HEp-2 cells infected with vBSΔ27 correlated with the appearance of the specific infected-cell phenotype observed in Fig. 1, infections were performed with HEp-2 cells as described above (Fig. 3) and the cell morphologies were documented at different times p.i. The results (Fig. 4) showed that at 6 and 9 h p.i., vBSΔ27-infected cells presented morphologies similar to those seen with KOS1.1-infected cells (compare Fig. 4A and B with Fig. 4F and G) or mock-infected cells (Fig. 4K and L). At 12 h p.i., some of the cells infected with vBSΔ27 showed a phenotype of small and irregular shapes (Fig. 4C). By 15 h p.i., the number of these "altered" cells had increased, reaching almost 100% at 24 h p.i. (Fig. 4D and E). The wild-type-infected monolayer presented the characteristics of more rounded cells generally associated with HSV-1-induced CPE (Fig. 4J).

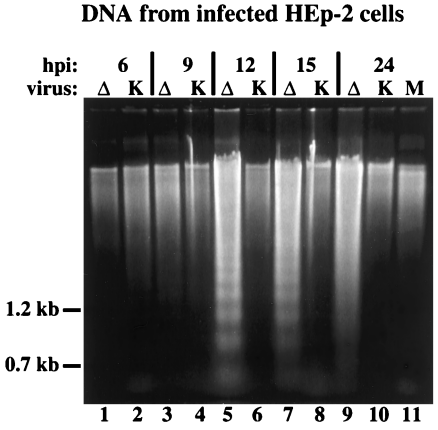

FIG. 5. Agarose gel electrophoresis of low-molecular-weight DNA extracted from infected HEp-2 cells. The DNAs were separated in a 1.5% agarose gel and stained with ethidium bromide after extraction at 6, 9, 12, 15, and 24 h p.i. from vBSΔ27 (Δ)- or KOS1.1 (K)-infected HEp-2 cells and at 24 h p.i. from mock (M)-infected HEp-2 cells as described in Materials and Methods. The locations of 1.2- and 0.7-kb markers are shown in the left margin.

The results shown in Fig. 4 confirm our original observations (Fig. 1). They also confirm our conclusion that the cytopathic process in HEp-2 cells induced by vBSΔ27 begins early in infection, since its effect on the morphologies of the infected cells (Fig. 4) and the levels of accumulation of viral proteins could be observed as early as 12 h p.i. (Fig. 3). Based on all of our findings (Fig. 1 to 4), we conclude that (i) vBSΔ27-infected HEp-2 cells were dying by a pathway different from that generally referred to as CPE, which occurs during wild-type infection, and in addition, (ii) this death pathway is specifically based on the origin of the cells, inasmuch as the phenotype did not occur in Vero cells or their derivative, Vero 2.2.

DNA fragmentation in vBSΔ27-infected HEp-2 cells. We have described a novel cytopathology which appeared to be specific to vBSΔ27-infected human cells. These cells could have died in one of many different ways, such as necrosis or a programmed cell death route like apoptosis. As discussed above, since the morphologies of the vBSΔ27-infected human cells differed from that of the wild-type control virus infections in the same cells, we concluded that necrosis leading to standard CPE was not the mechanism. Because we observed only a reduction of viral protein accumulations in the vBSΔ27-infected human cells, it was also unlikely that the cytopathology was due to a complete shutoff of protein synthesis, as can be observed in certain cells following infections with viruses that do not produce the $\gamma_1$34.5 protein (7, 13). Therefore, the goal of this series of experiments was to determine whether an apoptotic process might be the basis of our findings.

One characteristic feature of cells undergoing the final stages of apoptosis is the fragmentation of chromosomal DNA into nucleosomal oligomers (reviewed in reference 19). To test whether we could detect the presence of similar DNA fragmentation during the infection of HEp-2 cells by vBSΔ27, low-molecular-weight DNA was extracted at 6, 9, 12, 15, and 24 h p.i. from the cells shown in Fig. 4, separated in a 1.5% agarose gel, and stained as described in Materials and Methods. The results (Fig. 5) were as follows. (i) At 6 and 9 h p.i., essentially no differences were seen between the DNAs derived from vBSΔ27- and KOS1.1-infected cells (Fig. 5, lanes 1 to 4). (ii) Obvious DNA laddering patterns were observed at 12, 15, and 24 h p.i. with the vBSΔ27-infected cells (Fig. 5, lane 5, 7, and 9). The most pronounced pattern was seen at 12 h p.i., and by 24 h p.i., the pattern appeared more as a smear than a ladder. (iii) In all KOS1.1-infected cells and in mock-infected cells at 24 h p.i., such DNA laddering patterns were not observed (Fig. 5, lanes 6, 8, 10, and 11). Since the appearance of the genomic DNA fragmentation ladders coincided with the first observation of the small, irregular cell phenotypes in the vBSΔ27-infected HEp-2 cell monolayers (Fig. 4), we conclude that the two effects are the result of the same process. Together, these results suggest that vBSΔ27 induces apoptosis in the infected HEp-2 cells.

Chromatin condensation in vBSΔ27-infected HEp-2 cells. Cells undergoing apoptosis show characteristic morphologic changes, such as shrinkage, chromatin condensation, and nuclear fragmentation (19). Since the previous results indicated both cell shrinkage, as demonstrated by small, irregular cell shapes (Fig. 1 and 4), and genomic DNA laddering (Fig. 5) following vBSΔ27 infection of human cells, our goal was to observe the nuclei of these cells as well. vBSΔ27-, KOS1.1-, or mock-infected HEp-2 cells were stained with the Hoechst 33258 dye (Fig. 6) at 10 and 24 h p.i. as described in Materials and Methods.

At 10 h p.i., the vBSΔ27- and KOS1.1-infected cell nuclei showed similar staining patterns, which were spread throughout the nuclei (Fig. 6A and B). In contrast, at 24 h p.i. (Fig. 6E) almost all of the vBSΔ27-infected cell DNA staining patterns were much smaller and many appeared to be partitioned into several nodules. The DNA in these cells had an intense blue staining consistent with a condensation of the molecules that was different from that at 10 h p.i., which was diffused through the nuclei. The KOS1.1-infected cell nuclei at 24 h p.i. were bigger, with a more uniform blue staining (Fig. 6F). Some DNAs in these cells also showed a slightly brighter straining, but these DNAs appeared to be localized at the edges of the nuclei, suggestive of the margination of chromatin which was described earlier for wild-type infections (35). Uniform nuclear staining with no signs of condensation or margination was observed with the control mock-infected cells at 24 h p.i. All of the corresponding cell morphologies visualized by phase-contrast microscopy (Fig. 6C, D, H, I, and J) were identical to those presented earlier (Fig. 1 and 4).

All of our wild-type control infections of human cells showed features characteristic of CPEs leading to necrosis. Our results also showed that the vBSΔ27-infected HEp-2 cells had many of the characteristic features of apoptotic cells, such as shrinkage, chromatin condensation, and nuclear fragmentation. Based on these findings, we conclude that while both the wild-type and ICP27-null viruses likely induce an apoptotic event in infected human cells, the virus which lacks ICP27 was incapable of preventing this process from killing the cells. Since we did not observe the features of apoptosis in vBSΔ27-infected Vero cells, it appears that either (i) the virus does not induce this process in these cells, (ii) these cells might possess an activity which could compensate for the requirement for ICP27 and prohibit the process, or (iii) the cells themselves have lost their ability to proceed along the pathway leading to the induction of apoptosis.

Induction of apoptosis in HSV-1-infected cells. While many viruses are known to induce apoptosis in cells in response to infection (19), cells infected with wild-type HSV-1 do not show apoptotic features. An explanation for this apparent inconsistency was provided by Koyama and Adachi (20) when they showed that HSV-1 could, in fact, induce the characteristic morphological changes and endonucleosomal DNA cleavages of apoptosis when the infections were performed in HEp-2 cells in the presence of CHX, which inhibits all protein synthesis. To determine whether our findings were related to the

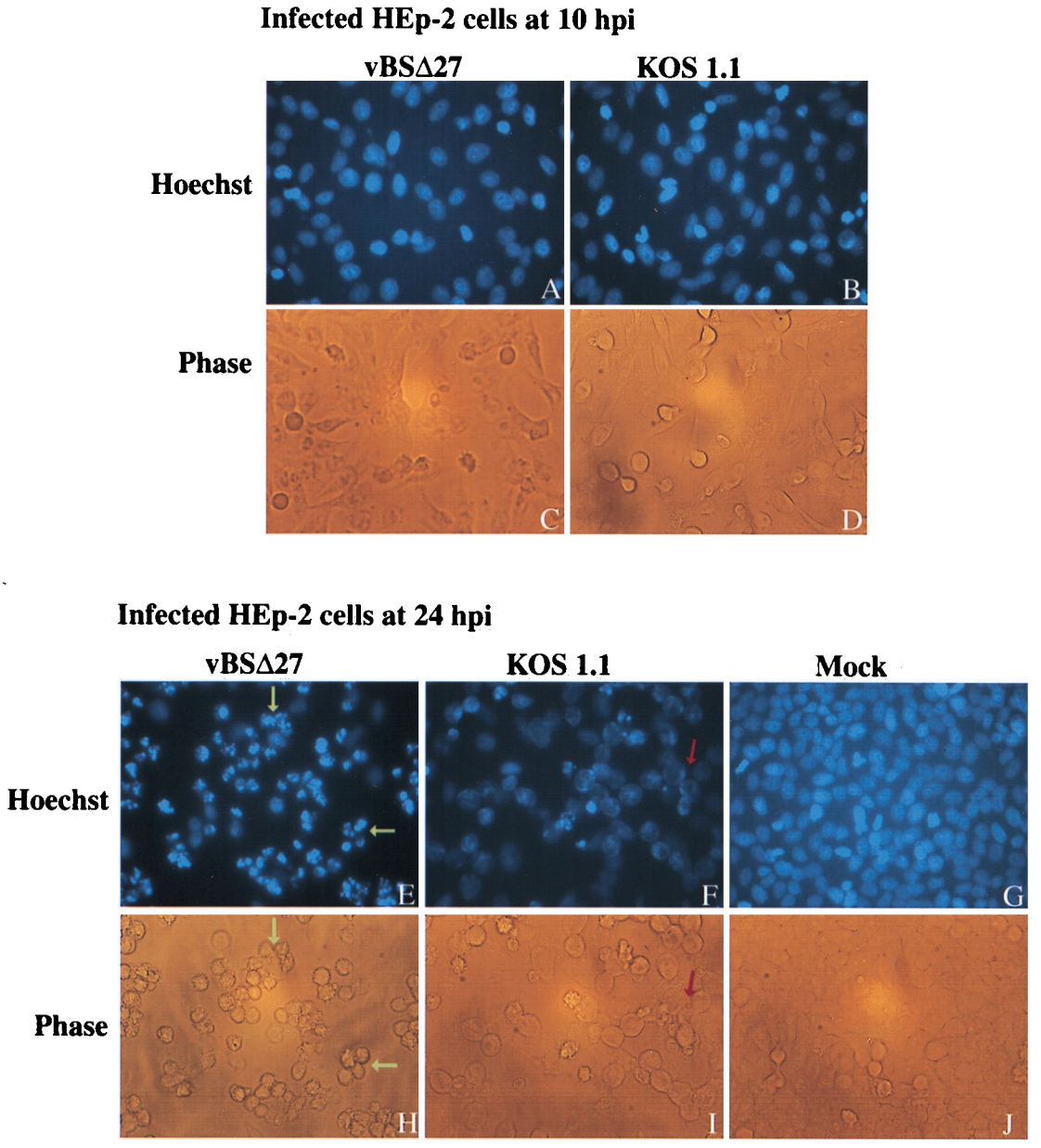

FIG. 6. Fluorescent visualization of infected HEp-2 cell DNA. Fluorescent images (Hoechst) and corresponding phase-contrast images (Phase) of HEp-2 cells at 10 or 24 h after infection with vBSΔ27 or KOS1.1 and 24 h after mock infection. The infected cells were stained with the Hoechst H33258 DNA dye as described in Materials and Methods. Yellow arrows, condensed chromatin; red arrow, marginal chromatin. Fluorescent and phase-contrast microscopy magnification, ×20.

effects described by Koyama and Adachi, two sets of studies were performed with HEp-2 and Vero cell monolayers infected in the absence or presence of CHX (20).

In the first series of experiments, comparisons of the morphologies of vBSΔ27- or wild-type virus (KOS1.1 and vBSΔ27R)-infected cells at 24 h p.i. were made (Fig. 7). In the absence of CHX, the control infections in Vero cells led to the typical CPE phenotype expected for the wild-type viruses (Fig. 7J and L). A phenotype very similar to that of mock-infected Vero cells was seen with vBSΔ27-infected Vero cells (compare Fig. 7I with Fig. 7K), as expected (44) (Fig. 1). When protein synthesis was inhibited by the addition of CHX, all infected cell monolayers looked similar to the corresponding mock-infected cells (Fig. 7M to P). Immunoblot analyses of these infected cells detected no viral proteins in the vBSΔ27-infected cells, and only very small amounts or no viral proteins were detected for the wild-type viruses (data not shown). Therefore, in Vero cells, even when protein synthesis was inhibited, the infected cells did not show any signs of apoptosis.

When the infections were performed in HEp-2 cells in the absence of CHX, previously described morphologies (Fig. 1) were seen which corresponded to the small, irregular cell phenotype for the vBSΔ27-infected cells (Fig. 7C) and standard CPE for the wild-type-infected cells (Fig. 7B and D). In contrast, when the infections were done in the presence of CHX, there was a reduction in the number of cells which remained attached to the dishes (data not shown) and all of the infected cells showed the same morphology, including small size, and

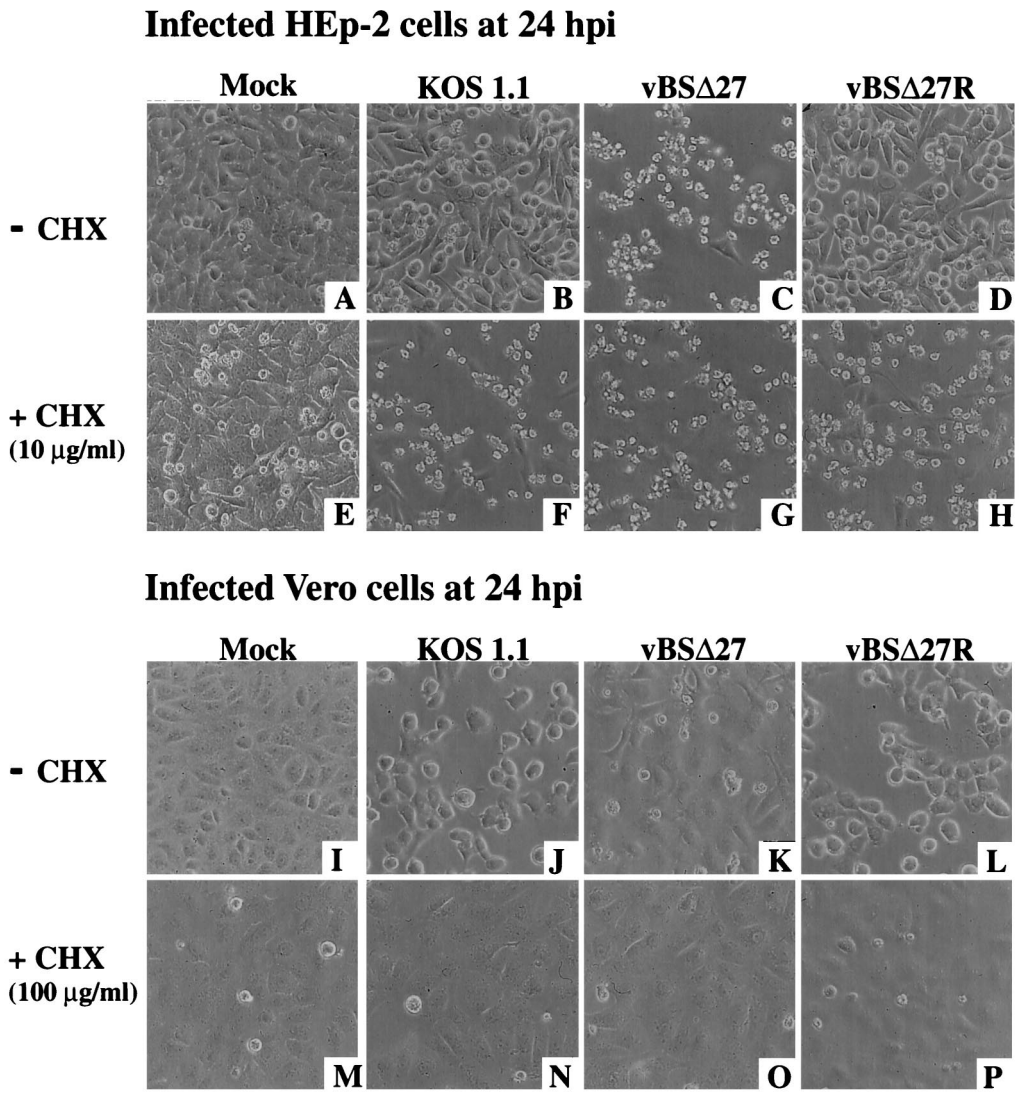

FIG. 7. Morphologies of HEp-2 and Vero cells at 24 h p.i. in the absence (−) or presence (+) of the protein synthesis inhibitor CHX. Phase-contrast images of HEp-2 (A to H) and Vero (I to P) cells mock infected or infected with KOS1.1, vBSΔ27, and vBSΔ27R are shown. Magnification, ×20. The CHX concentrations were 10 μg/ml for HEp-2 and 100 μg/ml for Vero cells.

irregular shaped features (Fig. 7F to H). Few cells in the mock-infected monolayer presented this latter phenotype, and the cells remained mostly flat and confluent (Fig. 7E). Thus, the addition of CHX to human cells infected with the wild-type viruses resulted in a cell phenotype identical to that which we described with vBSΔ27 in the absence of the drug.

In the second series of experiments (Fig. 8), HEp-2 cell infections in the presence of CHX were repeated and low-molecular-weight DNA was extracted at 6 and 15 h p.i. in order to look for genomic DNA laddering patterns shown in Fig. 5. DNA fragmentation was detected as early as 6 h p.i. in vBSΔ27- and KOS1.1-infected cells (Fig. 8A, lanes 2 and 3). The amounts of the DNA fragments isolated from these infected cells were higher at 15 h p.i. (Fig. 8B, lanes 1 and 2). No DNA laddering was observed with similarly infected Vero cells (data not shown). The cell morphologies were also observed prior to the DNA extractions. A higher number of cells with an apoptotic phenotype could be seen at 15 than at 6 h p.i. for the vBSΔ27- and KOS-infected cells (compare Fig. 8C and D with Fig. 8F and G). Thus, the increased amounts of DNA laddering detected in vBSΔ27- and KOS-infected HEp-2 cells correlated with an observed higher number of apoptotic cells. While some DNA laddering could be seen in the mock-infected lanes, the amounts were smaller than that observed for vBSΔ27 or KOS1.1 DNA (Fig. 8A and B) and the number of apoptotic cells (Fig. 8E) was not as high as with vBSΔ27- and KOS-infected cells at 15 h p.i.

Based on these results (Fig. 7 and 8), we conclude that the apoptosis which we have described in vBSΔ27-infected human cells was identical to that which occurs during wild-type infection of human cells when total protein synthesis has been inhibited. Therefore, it is conceivable that the effect of CHX was simply due to the absence of ICP27 in these cells.

DISCUSSION

Previous characterizations of the growth properties of mutant strains of HSV-1 which are unable to synthesize functional

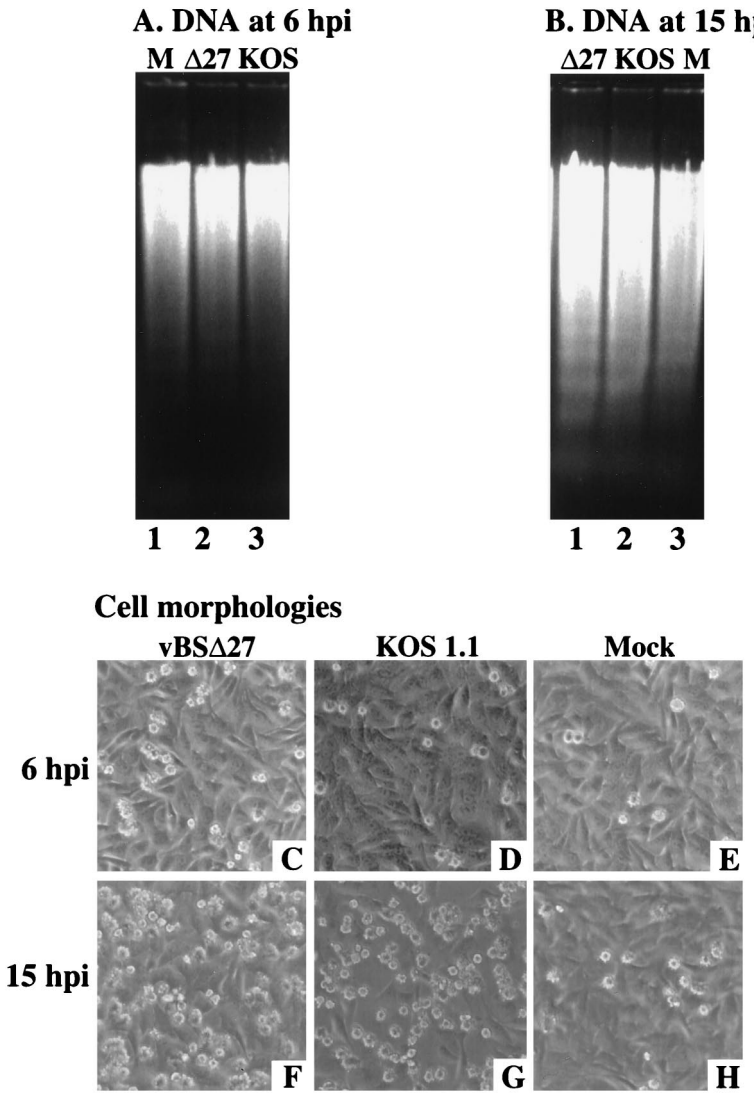

FIG. 8. Agarose gel electrophoresis of low-molecular-weight DNA (A and B) and morphologies (C to H) of HEp-2 cells infected in the presence of CHX. The DNAs were extracted at 6 and 15 h p.i. from vBSΔ27 (Δ27)-, KOS1.1-, or mock (M)-infected HEp-2 cells in the presence of 10 μg of CHX/ml and separated in 1.5% agarose gels. Phase-contrast images of the corresponding infected HEp-2 cells were taken prior to the DNA extractions. Magnification, ×20.

ICP27 have focused on infections in nonhuman Vero cells (25, 32, 37, 43–45). We set out to study the replication of an ICP27 deletion virus in several different strains of human cells. The significant findings of our study can be summarized as follows.

(i) We observed a novel human cell cytopathology following vBSΔ27 infections that was different from that seen with wild-type virus infections. Either KOS1.1 or vBSΔ27R (wild-type) infections of human cells produced large, rounded cells, consistent with classic CPE, while vBSΔ27 infections yielded small, irregular-shaped cells. In addition, this effect appeared to differ in human and nonhuman cells, since all vBSΔ27 infections of 143tk$^-$, HeLa, or HEp-2 cells produced the irregular-shaped cells while infection of Vero or Vero 2.2 cells did not. This finding was further supported by our recent preliminary results (1), which showed that rabbit skin cells appear to act similarly to the Vero and Vero 2.2 cells following vBSΔ27 infection.

(ii) Following vBSΔ27 infections of human cells, both IE and L viral proteins accumulated to lesser extents than those observed in either human cells infected with wild-type virus or vBSΔ27-infected Vero cells. Due to the possibility that specific viral proteins might be directly causing cell toxicity (17, 18, 38, 39, 46), we measured levels of protein accumulations rather than gene expression in the vBSΔ27-infected human cells. Since the amounts of viral proteins were simply reduced relative to the wild type and not eliminated, we concluded that direct toxicity was not the cause of our cytopathology. One unexpected finding following the vBSΔ27 infections was that while the IE ICP22 protein accumulated to levels higher than those observed with wild-type virus infection in Vero cells, few or no slower-migrating forms of ICP22 were seen with either the HEp-2 or Vero cells (Fig. 2 and 3). ICP22 was shown to be highly posttranslationally modified and it migrates as at least five forms in a one-dimensional denaturing gel (5, 6, 30). At least a portion of the modifications on ICP22 seem to require viral proteins made later in infection (30). These results suggest that the presence of ICP27 is required for the efficient posttranslational modification of ICP22 in all cells tested in this study.

(iii) We showed that the specific cytopathology observed in vBSΔ27-infected human cells was the consequence of apoptotic death. Our conclusion was based on our findings that vBSΔ27-infected human cells had small, irregular shapes suggestive of shrinkage, that their DNA was highly condensed in their nuclei, and that we were able to isolate low-molecular-weight DNAs from the cells which showed an oligosomal-sized laddering pattern in agarose gels. Together, these results suggest that while both the wild-type and ICP27-null viruses likely induce an apoptotic event in infected human cells, the virus which lacks ICP27 is incapable of preventing this process from killing the cells. It is of interest to note that our most pronounced DNA ladders were seen at 12 h p.i. and by 24 h p.i., the ladders appeared more as smears. Thus, in order to obtain definitive patterns, it is best to look earlier in infection rather than later. DNA laddering is perhaps the final observable consequence of apoptosis, and the fact that we could detect pronounced laddering at 12 h p.i. suggests that the induction of the process actually begins much earlier in infection.

(iv) ICP27 is required for the prevention of apoptosis in infected human cells. Our conclusion is based on the fact that apoptosis was observed only during infection with the vBSΔ27 virus. This is further supported by our recent results (1), which also demonstrated apoptosis in human cells following infection at the nonpermissive temperature with the vBSLG4 virus, which synthesizes a temperature-sensitive form of ICP27 (44). ICP27 is a multifunctional regulatory phosphoprotein which can associate with other viral regulatory proteins (27, 48) and is required for optimal DNA synthesis and the expression of some viral L genes (25, 32, 37, 43–45). Recently, it was shown that ICP27 inhibits host cell splicing, redistributes splicing components throughout the nucleus, and aids in the export of RNA from the nucleus (12, 26, 28, 40, 41). Based on our current data, we are unable to assess whether one of these known functions of ICP27 is also involved in the prevention of apoptosis. Experiments focusing on the role of ICP27 alone in response to various stimuli of apoptosis should help answer these questions.

Also, we do not know whether ICP27 itself is directly involved in blocking apoptosis or whether another viral component, whose production or activity is dependent on ICP27, plays a role. At least two viral proteins which might act to prevent apoptosis are produced later than ICP27. Although the $\gamma_1$34.5 protein was already shown to block the complete shutoff of protein synthesis in HSV-1 infected-cells (7, 13), no signs of apoptosis were reported in cells infected with viruses unable to synthesize this protein. In addition, we observed a reduction in IE and L protein accumulation, not a complete turnoff of protein synthesis, indicating that the $\gamma_1$34.5 protein was likely active in the vBSΔ27-infected human cells. The U_S3 protein kinase was also reported to be required for the inhibition of apoptosis (23). Since the level of VP16 (model L [γ_1] protein) was reduced in vBSΔ27-infected human cells, it is likely that the level of accumulation of U_S3 (E protein) was also reduced during our vBSΔ27 infections of human cells. In addition, if this protein is contained within the virion (31), that might explain why we were unable to observe the apoptotic effects on the human cells until at least 9 to 10 h p.i. (Fig. 4).

(v) The apoptosis in vBSΔ27-infected human cells was identical to that observed in human cells following infection with wild-type virus in the presence of CHX. This suggests that the effect of CHX is simply due to the absence of ICP27 in these cells. However, regardless of the virus, the infected Vero and Vero 2.2 cells did not show any signs of apoptosis when protein synthesis was inhibited by CHX. This finding raises the question of whether Vero cells can undergo apoptosis upon treatment with the inhibitor. Our results showing that we did not observe cell morphological changes or DNA laddering in the presence of CHX seem to support this theory. Additional support for this model comes from the observation that while HeLa cells undergo apoptosis when exposed to metabolic inhibitors, baby hamster kidney cells and a number of other cells are protected (24). However, Galvan and Roizman (10) showed the induction of apoptosis in Vero cells following other treatments. These authors also concluded that the ability of HSV-1 mutants to induce apoptosis was cell type dependent, suggesting that induction could involve multiple and diverse viral gene products (10). Although the Vero cells used in this study were passaged less than 140 times after isolation from tissue, we cannot exclude the possibility that the absence of apoptosis in these cells is a consequence of some alteration that evolved during their passage in the laboratory.

Although the induction of apoptosis by HSV-1 is expected to involve the interaction of viral proteins with cellular components, it is possible that such cellular products differ in their abundance or activity in various types of cells. Our results suggest that while HSV-1 infection likely induces apoptosis in all cells, viral evasion of the response differs among the cells tested in this study. Consideration of these findings would be beneficial to those characterizing mutant recombinant viruses, since they emphasize the importance of testing all relevant cell lines for cytopathic phenotypes during the course of productive viral infection.

ACKNOWLEDGMENTS

We thank (i) Saul Silverstein and Bob Soliman (Columbia) for graciously providing the HSV-1(KOS1.1), HSV-1(vBSΔ27), HSV-1 (vBSΔ27)R, and HSV-1(vBSLG4) viruses and Vero 2.2 cells used in this study; (ii) Rozanne Sandri-Goldin (UC—Irvine), from whom the Vero 2.2 cells were originally obtained; (iii) Lisa Pomeranz (MSSM) for discussions and expert advice regarding the fluorescent-microscopy experiments; and (iv) Jennifer O'Toole (MSSM) for expert technical help.

These studies were supported in part by grants from the United States Public Health Service (AI38873) and the American Cancer Society (JFRA 634) and an unrestricted grant from the National Foundation for Infectious Diseases. J.A.B. is a Markey Research Fellow and thanks the Lucille P. Markey Charitable Trust for their support.

REFERENCES

1. **Aubert, M., and J. A. Blaho.** Unpublished data.
2. **Avitabile, E., S. Di Gaeta, M. R. Torrisi, P. L. Ward, B. Roizman, and G. Campadelli-Fiume.** 1995. Redistribution of microtubules and Golgi apparatus in herpes simplex virus-infected cells and their role in viral exocytosis. J. Virol. **69:**7472–7482.
3. **Bates, P. A., and N. A. DeLuca.** 1998. The polyserine tract of herpes simplex virus ICP4 is required for normal viral gene expression and growth in murine trigeminal ganglia. J. Virol. **72:**7115–7124.
4. **Batterson, W., and B. Roizman.** 1983. Characterization of the herpes simplex virion-associated factor responsible for the induction of alpha genes. J. Virol. **46:**371–377.
5. **Blaho, J. A., C. Mitchell, and B. Roizman.** 1993. Guanylylation and adenylylation of the alpha regulatory proteins of herpes simplex virus require a viral beta or gamma function. J. Virol. **67:**3891–3900.
6. **Blaho, J. A., C. S. Zong, and K. A. Mortimer.** 1997. Tyrosine phosphorylation of the herpes simplex virus type 1 regulatory protein ICP22 and a cellular protein which shares antigenic determinants with ICP22. J. Virol. **71:**9828–9832.
7. **Chou, J., and B. Roizman.** 1992. The gamma 1(34.5) gene of herpes simplex virus 1 precludes neuroblastoma cells from triggering total shutoff of protein synthesis characteristic of programmed cell death in neuronal cells. Proc. Natl. Acad. Sci. USA **89:**3266–3270.
8. **Chou, J., J. J. Chen, M. Gross, and B. Roizman.** 1995. Association of a M(r) 90,000 phosphoprotein with protein kinase PKR in cells exhibiting enhanced phosphorylation of translation initiation factor eIF-2 alpha and premature shutoff of protein synthesis after infection with $\gamma_1$34.5− mutants of herpes simplex virus 1. Proc. Natl. Acad. Sci. USA **92:**10516–10520.
9. **Fenwick, M. L., and M. J. Walker.** 1978. Suppression of the synthesis of

cellular macromolecules by herpes simplex virus. J. Gen. Virol. **41:**37–51.
10. **Galvan, V., and B. Roizman.** 1998. Herpes simplex virus 1 induces and blocks apoptosis at multiple steps during infection and protects cells from exogenous inducers in a cell-type-dependent manner. Proc. Natl. Acad. Sci. USA **95:**3931–3936.
11. **Hampar, B., and S. A. Elison.** 1961. Chromosomal aberrations induced by an animal virus. Nature **192:**145–147.
12. **Hardy, R. W., and R. M. Sandri-Goldin.** 1994. Herpes simplex virus inhibits host cell splicing and the regulatory protein ICP27 is required for this effect. J. Virol. **68:**7790–7799.
13. **He, B., J. Chou, R. Brandimarti, I. Mohr, Y. Gluzman, and B. Roizman.** 1997. Suppression of the phenotype of $\gamma_1$34.5$^-$ herpes simplex virus 1: failure of activated RNA-dependent protein kinase to shut off protein synthesis is associated with a deletion in the domain of the α47 gene. J. Virol. **71:**6049–6054.
14. **Heeg, U., H. P. Dienes, S. Muller, and D. Falke.** 1986. Involvement of actin-containing microfilaments in HSV-induced cytopathology and the influence of inhibitors of glycosylation. Arch. Virol. **91:**257–270.
15. **Honess, R. W., and B. Roizman.** 1974. Regulation of herpesvirus macromolecular synthesis. I. Cascade regulation of the synthesis of three groups of viral proteins. J. Virol. **14:**8–19.
16. **Honess, R. W., and B. Roizman.** 1975. Regulation of herpesvirus macromolecular synthesis: sequential transition of polypeptide synthesis requires functional viral polypeptides. Proc. Natl. Acad. Sci. USA **72:**1276–1280.
17. **Johnson, P. A., A. Miyanohara, F. Levine, T. Cahill, and T. Friedmann.** 1992. Cytotoxicity of a replication-defective mutant of herpes simplex virus type 1. J. Virol. **66:**2952–2965.
18. **Johnson, P. A., M. J. Wang, and T. Friedmann.** 1994. Improved cell survival by the reduction of immediate-early gene expression in replication-defective mutants of herpes simplex virus type 1 but not by mutation of the virion host shutoff function. J. Virol. **68:**6347–6362.
19. **Kerr, F. R., and B. V. Harmon.** 1991. Definition and incidence of apoptosis: an historical perspective, p. 5–29. *In* L. D. Tomei and F. O. Cope (ed.), Apoptosis: the molecular basis of cell death. Cold Spring Harbor Laboratory, Cold Spring Harbor, N.Y.
20. **Koyama, A. H., and A. Adachi.** 1997. Induction of apoptosis by herpes simplex virus type 1. J. Gen. Virol. **78:**2909–2912.
21. **Koyama, A. H., and Y. Miwa.** 1997. Suppression of apoptotic DNA fragmentation in herpes simplex virus type 1-infected cells. J. Virol. **71:**2567–2571.
22. **Leopardi, R., and B. Roizman.** 1996. The herpes simplex virus major regulatory protein ICP4 blocks apoptosis induced by the virus or by hyperthermia. Proc. Natl. Acad. Sci. USA **93:**9583–9587.
23. **Leopardi, R., C. Van Sant, and B. Roizman.** 1997. The herpes simplex virus 1 protein kinase U_S3 is required for protection from apoptosis induced by the virus. Proc. Natl. Acad. Sci. USA **94:**7891–7896.
24. **Martin, D. P., R. E. Schmidt, P. S. DiStefano, O. H. Lowry, J. G. Carter, and E. M. Johnson, Jr.** 1988. Inhibitors of protein synthesis and RNA synthesis prevent neuronal death caused by nerve growth factor deprivation. J. Cell Biol. **106:**829–844.
25. **McCarthy, A. M., L. McMahan, and P. A. Schaffer.** 1989. Herpes simplex virus type 1 ICP27 deletion mutants exhibit altered patterns of transcription and are DNA deficient. J. Virol. **63:**18–27.
26. **Mears, W. E., and S. A. Rice.** 1998. The herpes simplex virus immediate-early protein ICP27 shuttles between nucleus and cytoplasm. Virology **242:**128–137.
27. **Panagiotidis, C. A., E. K. Lium, and S. J. Silverstein.** 1995. Physical and functional interactions between herpes simplex virus immediate-early proteins ICP4 and ICP27. J. Virol. **71:**1547–1557.
28. **Phelan, A., M. Carmo-Fonseca, J. McLauchlan, A. I. Lamond, and J. B. Clements.** 1993. A herpes simplex virus type 1 immediate-early gene product, IE63, regulates small nuclear ribonucleoprotein distribution. Proc. Natl. Acad. Sci. USA **90:**9056–9060.
29. **Post, L. E., and B. Roizman.** 1981. A generalized technique for deletion of specific genes in large genomes: α gene 22 of herpes simplex virus 1 is not essential for growth. Cell **25:**227–232.
30. **Purves, F. C., W. O. Ogle, and B. Roizman.** 1993. Processing of the herpes simplex virus regulatory protein alpha 22 mediated by the UL13 protein kinase determines the accumulation of a subset of alpha and gamma mRNAs and proteins in infected cells. Proc. Natl. Acad. Sci. USA **90:**6701–6705.
31. **Read, G. S., and N. Frenkel.** 1983. Herpes simplex virus mutants defective in the virion-associated shutoff of host polypeptide synthesis and exhibiting abnormal synthesis of α (immediate early) viral polypeptides. J. Virol. **46:**498–512.
32. **Rice, S. A., and D. M. Knipe.** 1990. Genetic evidence for two distinct transactivation functions of the herpes simplex virus alpha protein ICP27. J. Virol. **64:**1704–1715.
33. **Roizman, B.** 1962. Polykaryocytosis induced by viruses. Proc. Natl. Acad. Sci. USA **48:**228–234.
34. **Roizman, B., and P. R. Roanne.** 1964. Multiplication of herpes simplex virus. II. The relationship between protein synthesis and the duplication of viral DNA in infected HEp-2 cells. Virology **22:**262–269.
35. **Roizman, B., and D. Furlong.** 1974. The replication of herpesviruses, p. 229–403. *In* H. Fraenkel-Conrat and R. R. Wagner (ed.), Comprehensive virology. Plenum, New York, N.Y.
36. **Roizman, B., and A. Sears.** 1996. Herpes simplex viruses and their replication, p. 2231–2295. *In* B. N. Fields and D. M. Knipe (ed.), Virology, 3rd ed., Lippincott-Raven, Philadelphia, Pa.
37. **Sacks, W. R., C. C. Greene, D. P. Aschman, and P. A. Schaffer.** 1985. Herpes simplex type 1 ICP27 is an essential regulatory protein. J. Virol. **55:**796–805.
38. **Samaniego, L. A., N. Wu, and N. A. DeLuca.** 1997. The herpes simplex virus immediate-early protein ICP0 affects transcription from the viral genome and infected-cell survival in the absence of ICP4 and ICP27. J. Virol. **71:**4614–4625.
39. **Samaniego, L. A., L. Neiderhiser, and N. A. DeLuca.** 1998. Persistence and expression of the herpes simplex virus genome in the absence of immediate-early proteins. J. Virol. **72:**3307–3320.
40. **Sandri-Goldin, R. M., and G. E. Mendoza.** 1992. A herpes virus regulatory protein appears to act posttranscriptionally by affecting mRNA processing. Genes Dev. **6:**848–863.
41. **Sandri-Goldin, R. M., M. K. Hibbard, and M. A. Hardwicke.** 1995. The C-terminal repressor region of herpes simplex type 1 ICP27 is required for redistribution of small nuclear ribonucleoprotein particles and splicing factor SC35; however, these alterations are not sufficient to inhibit host cell splicing. J. Virol. **69:**6063–6076.
42. **Sears, A. E., I. W. Halliburton, B. Meignier, S. Silver, and B. Roizman.** 1985. Herpes simplex virus 1 mutant deleted in the α22 gene: growth and gene expression in permissive and restrictive cells and establishment of latency in mice. J. Virol. **55:**338–346.
43. **Sekulovich, R. E., K. Leary, and R. M. Sandri-Goldin.** 1988. The herpes simplex virus type 1 alpha protein ICP27 can act as a *trans*-repressor or a *trans*-activator in combination with ICP4 and ICP0. J. Virol. **62:**4510–4522.
44. **Soliman, T. M., R. M. Sandri-Goldin, and S. J. Silverstein.** 1997. Shuttling of the herpes simplex type 1 regulatory protein ICP27 between the nucleus and cytoplasm mediates the expression of late proteins. J. Virol. **71:**9188–9197.
45. **Uprichard, S. L., and D. M. Knipe.** 1996. Herpes simplex ICP27 mutant viruses exhibit reduced expression of specific DNA replication genes. J. Virol. **70:**1969–1980.
46. **Wu, N., S. C. Watkins, P. A. Schaffer, and N. A. DeLuca.** 1996. Prolonged gene expression and cell survival after infection by a herpes simplex virus mutant defective in the immediate-early genes encoding ICP4, ICP27, and ICP22. J. Virol. **70:**6358–6369.
47. **Xia, K., D. K. Knipe, and N. A. DeLuca.** 1996. Role of protein kinase A and the serine-rich region of herpes simplex virus type 1 ICP4 in viral replication. J. Virol. **70:**1050–1060.
48. **Zhu, Z., and P. A. Schaffer.** 1995. Intracellular localization of the herpes simplex virus type 1 major transcriptional regulatory protein, ICP4, is affected by ICP27. J. Virol. **69:**49–59.